J. Fluid Mech. (1996), vol. 326, pp. 357–372



# Self-similarity of decaying two-dimensional turbulence

By PETER BARTELLO[1] AND TOM WARN[2]

[1]Recherche en Prévision Numérique, Atmospheric Environment Service, 2121 voie de Service nord, Route Transcanadienne, Dorval (Québec) H9P 1J3, Canada

[2]Department of Atmospheric and Oceanic Sciences, McGill University, 805 Sherbrooke Street West, Montreal, (Québec) H3A 2K6, Canada

(Received 28 December 1995 and in revised form 11 June 1996)

Simulations of decaying two-dimensional turbulence suggest that the one-point vorticity density has the self-similar form

$$p_\omega \sim t\, f(\omega t)$$

implied by Batchelor's (1969) similarity hypothesis, except in the tails. Specifically, similarity holds for $|\omega| < \omega_m$, while $p_\omega$ falls off rapidly above. The upper bound of the similarity range, $\omega_m$, is also nearly conserved in high-Reynolds-number hyperviscosity simulations and appears to be related to the average amplitude of the most intense vortices (McWilliams 1990), which was an important ingredient in the vortex scaling theory of Carnevale *et al.* (1991).

The universal function $f$ also appears to be hyperbolic, i.e.

$$f(x) \sim c/2|x|^{1+q_c},$$

for $|x| > x^*$, where $q_c \doteq 0.4$ and $x^* \doteq 70$, which along with the truncated similarity form implies a phase transition in the vorticity moments

$$\langle|\omega|^q\rangle \sim \begin{cases} c_q\, t^{-q}, & -1 < q < q_c \\ c\,(q-q_c)^{-1}\, \omega_m^{q-q_c}\, t^{-q_c}, & q > q_c, \end{cases}$$

between the self-similar 'background sea' and the coherent vortices. Here $c_q$ and $c$ are universal. Low-order moments are therefore consistent with Batchelor's similarity hypothesis whereas high-order moments are similar to those predicted by Carnevale *et al.* (1991). A self-similar but less well-founded expression for the energy spectrum is also proposed.

It is also argued that $\omega_s = x^*/t$ represents 'mean sea-level', i.e. the (average) threshold separating the vortices and the sea, and that there is a spectrum of vortices with amplitudes in the range $(\omega_s, \omega_m)$. The total area occupied by vortices is also found to remain constant in time, with losses due to mergers of large-amplitude vortices being balanced by gains due to production of weak vortices. By contrast, the area occupied by vortices above a *fixed* threshold decays in time as observed by McWilliams (1990).

## 1. Introduction

### 1.1. *Fundamentals*

According to the two-dimensional Navier–Stokes equations

$$\frac{\mathrm{d}\mathscr{E}}{\mathrm{d}t} = -\nu\mathscr{Z}_2 \qquad \text{and} \qquad \frac{\mathrm{d}\mathscr{Z}_q}{\mathrm{d}t} = -\nu q(q-1)\langle|\omega|^{q-2}\nabla\omega\cdot\nabla\omega\rangle$$

for $q > 1$ for horizontally homogeneous incompressible flow, where

$$\mathscr{E} = \langle v_i(\mathbf{x})v_i(\mathbf{x})\rangle/2 \qquad \text{and} \qquad \mathscr{Z}_q = \langle|\omega(\mathbf{x})|^q\rangle.$$

Energy and (all) vorticity moments are therefore conserved when $\nu = 0$, while energy and moments of order $q \geqslant 1$ decay when $\nu \neq 0$. Here, $v_i$ and $\omega$ are the velocity and vorticity, while angle brackets denote ensemble averages. Furthermore, since the enstrophy $\mathscr{Z} = \mathscr{Z}_2/2$ is bounded by its initial value in two-dimensional turbulence, the energy dissipation vanishes and energy conservation is recovered in the limit $\nu \to 0$. Energy is therefore sometimes said to be a rugged invariant (although the terminology varies). Also, since vorticity contours are stretched in compex flows, vorticity gradients amplify so that all positive-order vorticity moments appear to dissipate in the small-viscosity limit.

### 1.2. *Batchelor's similarity theory*

The observation that energy is a rugged invariant whereas positive-order vorticity moments probably decay prompted Batchelor (1969) to hypothesize that outside the dissipation range and after sufficient time, high-Reynolds-number decaying two-dimensional turbulence depends only on $\mathscr{E}$ and $t$. In this case the only velocity, length, and time scales are

$$U = \mathscr{E}^{1/2}, \qquad L = Ut \qquad \text{and} \qquad T = t$$

so the energy spectrum, defined by

$$\mathscr{E} = \int_0^\infty E(k,t)\,\mathrm{d}k,$$

takes the form

$$E(k,t) \sim U^3 t\, F(kUt) \quad \text{for} \quad k \ll k_d \tag{1.1}$$

as $t \to \infty$, where $k_d$ is the dissipation wavenumber and $F$ is a universal function. Energy is therefore predicted to cascade upscale.

Batchelor's hypothesis has other implications. The one-point vorticity density is predicted to have the self-similar form

$$p_\omega(\omega,t) \sim t\, f(\omega t), \tag{1.2}$$

for some symmetric universal function $f$, while

$$\langle|\omega|^q\rangle \sim c_q t^{-q}, \tag{1.3}$$

where $c_q$ is a universal function of $q$ (the moments of $f$). The density therefore narrows with time while positive-order moments decay like $t^{-q}$. The predicted density is also 'super universal' in the sense that it is *completely independent of the flow state.* By contrast, the one-point velocity density is predicted to take the form

$$p_u(v,t) \sim g(v/U)/U, \tag{1.4}$$

where $g$ is a (symmetric) universal function, while

$$\langle |v|^q \rangle \sim a_q U^q.$$

The velocity statistics are therefore fixed by the energy and are predicted to be invariant in time. As far as we are aware (1.2) and (1.4) remain untested.

Strictly speaking, Batchelor's hypothesis applies only to unbounded flows since the inverse cascade must be arrested on finite or doubly periodic domains and the domain size $D$ becomes important. It is expected to describe the intermediate asymptotics when $L/D \ll 1$ initially however, where $L$ represents the energy-containing scale.

According to Batchelor's hypothesis $L \sim Ut$, implying that the Reynolds number $Re = UL/\nu$ increases with time so that energy conservation in the limit $t \to \infty$ cannot be ruled out, even if the initial Reynolds number is finite. In this case the final, rather than the initial, energy should control the long-term behaviour. Energy conservation at large times is also consistent in that the enstrophy decay law gives the energy dissipation $c_2\nu/t^2$ and a finite energy loss over the interval $(t, \infty)$ that is independent of $U$. In other words, Batchelor's hypothesis suggests that finite-Reynolds-number flows on unbounded domains do not approach a state of rest as $t \to \infty$ as do doubly periodic or bounded flows.

Numerical studies of decaying two-dimensional turbulence beginning with Lilly (1969) have confirmed that energy and enstrophy are transferred to large and small scales respectively, while subsequent studies have shown that an initially random vorticity field organizes into a collection of vortices on a background 'sea of vorticity' which gradually increase in scale and diminish in number through a complicated sequence of mergers (Fornberg 1977; Basedvant *et al.* 1981; McWilliams 1984, 1990; Benzi, Patarnello & Santangelo 1987). The vortices are coherent in the sense that their lifetimes are long compared to their recirculation times and become progressively more isolated with time, behaving in some respects like a collection of point vortices (Benzi *et al.* 1987, 1988, 1992; Carnevale, Pomeau & Young 1990; Carnevale *et al.* 1991; Weiss & McWilliams 1993). The statistical properties of the vortices also appear to depend on the nature of the initial conditions (Santangelo, Benzi & Legras 1989).

The observed self-organization and depletion of nonlinearities within the vortex cores undermines Batchelor's similarity theory (McWilliams 1990; Carnevale *et al.* 1991). In particular (1.3) with $q = 2$ considerably overestimates the enstrophy decay rate. In other words (1.2) appears to fail as does (1.1) in view of the relation

$$\mathscr{Z} = \int_0^\infty k^2 E(k,t)\,\mathrm{d}k.$$

Since extrema of the vorticity field are bounded by their initial values, the failure of (1.2) for large $\omega$ is inevitable if the vorticity of each realization is bounded initially, since the tails of the distribution cannot be universal. The extent to which this disrupts the similarity of the moments depends on the nature of the tails.

### 1.3. *Vortex theory of Carnevale et al.*

On the basis of a 'vortex census' McWilliams (1990) and Carnevale *et al.* (1991) suggested that Batchelor's hypothesis fails because of the existence of a second asymptotic invariant, $\zeta_{ext}$, which is characteristic of the amplitude of the most intense vortices. This is plausible given that the vortices grow in size and become increasingly sparse if a subset of the vortices either escapes interaction altogether or if their cores are protected from deformations and dissipation during interactions.

They also noted that when the emerging vortex population has narrowly distributed properties, then the long-time flow has the form of a dilute vortex gas consisting of vortices of amplitude $\zeta_{ext}$ and radius $a$ and that

$$\mathscr{E} \sim \rho a^4 \zeta_{ext}^2 \quad \text{and} \quad Z_q \sim \rho a^2 \zeta_{ext}^q,$$

where $\rho$ is the number density. Conservation of $\mathscr{E}$ and $\zeta_{ext}$ and the numerically observed scaling law

$$\rho \sim t^{-\xi},$$

where $\xi \doteq 0.75$ (McWilliams 1990)† then imply

$$a \sim t^{\xi/4}$$

and

$$Z_q \sim \zeta_{ext}^q t^{-\xi/2}. \tag{1.5}$$

Since

$$\rho a^2 \sim t^{-\xi/2},$$

the fractional area occupied by the vortices is predicted to decrease with time. The enstrophy decay rate is also slower than implied by (1.3) as observed, and the decay rates of all moments are predicted to be independent of their order. The latter remains to be verified. Our simulations suggest that this is the case when $q > \xi/2$.

Weiss & McWilliams (1993) also present evidence that (1.5) holds even when $\zeta_{ext}$ decays (slowly) because of finite Reynolds number effects. In particular they found that when the observed decay

$$\zeta_{ext} \sim t^{-\eta}$$

is accounted for in (1.5), then

$$\mathscr{Z} \sim t^{-(2\eta+\xi/2)},$$

which was in closer agreement with the simulations.

Questions remain however, particularly regarding the role of the 'sea' and the extent to which the vortex population remains narrowly distributed as $t \to \infty$. Also, no dimensionally consistent expression of the form (1.5) can be constructed from the invariants and time alone, suggesting that it is either incorrect or the parameter set $\mathscr{E}$, $t$ and $\zeta_{ext}$ is incomplete.

### 1.4. *Generalized similarity*

If indeed there is a second asymptotic invariant as suggested by McWilliams' (1990) vortex census, then it can be used to generalize Batchelor's similarity theory provided it can be represented in terms of more conventional statistical quantities. One possibility is

$$\omega_m(t) = Z_{q+1}/Z_q,$$

which according to (1.5) is proportional to $\zeta_{ext}$ as $t \to \infty$ and so should also be invariant. Alternatively

$$\omega_m(t) = \lim_{q\to\infty} Z_q^{1/q}$$

might be invariant, athough this is more delicate and less certain due to its sensitivity to the tails of the distribution.

† Huber & Alstrøm (1993) suggest this may be exact.

When Batchelor's hypothesis is generalized to include $\omega_m$, it leads to the additional time and length scales

$$\omega_m^{-1} \qquad \text{and} \qquad U/\omega_m,$$

while (1.1), (1.2) and (1.4) are replaced by

$$E(k,t) \sim U^3 t\, F(kUt, \omega_m t), \tag{1.6}$$

$$p_\omega \sim t\, f(\omega t, \omega/\omega_m) \tag{1.7}$$

and

$$p_u(v,t) \sim g(v/U, \omega_m t)/U. \tag{1.8}$$

Unfortunately these are not particularly informative. Progress is possible however, essentially because simulations suggest that (1.7) may have a simple dependence on $\omega_m$.

## 2. Numerical simulations

### 2.1. *Description of simulations*

Simulations using a (de-aliased) pseudo-spectral code have been performed at various resolutions, although only the highest which use $1024^2$ collocation points will be presented. Even this is barely adequate given that the energy in the first decade must be kept small to avoid finite-domain effects, while the last decade must be reserved for the dissipation range. For most of the discussion below we will employ direct simulations of the Navier–Stokes equations. However, as noted in previous studies, the resolvable Reynolds numbers are simply too low to obtain convincing evidence for a second invariant unless some form of hyperviscosity is used, i.e. simulations based on

$$\frac{\mathrm{d}\omega}{dt} = (-1)^{p+1} \nu_p \nabla^{2p} \omega.$$

Here we use $p = 8$. Hyperviscosity has the advantage of compressing the dissipation range, presumably allowing a higher effective Reynolds number at a given resolution (although Reynolds numbers are difficult to compare). It has the disadvantage that vorticity extrema no longer decay *a priori* since the viscous flux of vorticity is no longer proportional to the vorticity gradient (McWilliams 1990; Mariotti, Legras & Dritschel 1994). We also find that the scaling properties deteriorate somewhat, perhaps because of the increased variability. The overall behaviour of the two simulations is similar however, but since there are differences, it seems best to regard them as distinct candidates for similarity, possibly with different universal behaviour.

The simulated flow is doubly periodic on a square of sides $2\pi$ so that care must be taken to ensure it does not become 'boxed in' in the sense that the domain size becomes significant, arrests the inverse cascade and spoils similarity. Ideally energy should be confined to high wavenumbers throughout the simulation, although this is difficult to ensure because of the upscale energy transfer. Evidently

$$\left(\mathscr{L}/\mathscr{E}\right)^{1/2} \gg 1$$

is a necessary condition for the domain size to be unimportant. The Navier–Stokes integration was stopped after about 150 turnover times (see below) since this was no longer satisfied. The hyperviscosity run was stopped after about 300 turnover times, essentially because of excessive computation time. (The evolution slows with time so the sampling times must increase exponentially to observe significant changes.)

| $T_i$ | $\mathscr{E}$ | $\mathscr{Z}$ | $N_t$ |
|---|---|---|---|
| 0 | 2.55 | 10000 | 0 |
| 0.21 | 1.96 | 2826 | 16 |
| 0.45 | 1.55 | 1119 | 26 |
| 0.99 | 1.35 | 390 | 40 |
| 2.18 | 1.18 | 137 | 57 |
| 4.63 | 1.07 | 50 | 79 |
| 9.93 | 0.97 | 19 | 108 |
| 20.91 | 0.89 | 7 | 146 |

TABLE 1. Navier–Stokes simulation ($\nu = 3 \times 10^{-4}$).

In both simulations the initial energy spectrum is taken as

$$E(k,0) = a \begin{cases} k^{10} & \text{when } k < k_i \\ k_i^{20}/k^{10} & \text{when } k \geqslant k_i, \end{cases} \tag{2.1}$$

with $k_i = 60$ and random phases. The normalization constant was chosen so that $\mathscr{Z} = 10^4$ initially, which gives $\mathscr{E}$ of order unity. Since the time step is limited by $[Uk_{max}]^{-1}$, the number of steps per global turnover time $\mathscr{Z}^{-1/2}$

$$\mathscr{N} \approx (\mathscr{E}/\mathscr{Z})^{1/2} k_{max}$$

is fairly small initially and the early evolution is relatively fast. By the end of the simulation, $\mathscr{N}$ increases by an order of magnitude and the evolution slows considerably.

Since ensemble averages are estimated by area averages, they are strictly reliable only when the integral scale is much less than the domain size, which is certainly not the case near the end of the simulation. Tests at lower resolutions suggest that the scaling properties of the moments are much more robust than the moments themselves however, provided sampling error does not get completely out of control.

### 2.2. *Preliminary results*

Certain global statistics for the Navier–Stokes simulation at $t = 0$ and seven approximately logarithmically spaced ouput times $T_i$ are presented in table 1. The Reynolds number of the energy-containing scale varies from a few hundred initially to around 10000 by the end of the run. Also included is the integrated number of eddy turnover times

$$N_t = \int_0^t \mathscr{Z}(t')^{1/2} \, \mathrm{d}t',$$

which gives a useful measure of the elapsed time for decaying turbulence, The degree to which the flow has organized into a collection of vortices can be seen in figure 1.

Both energy and enstrophy decay throughout the simulation because of the limited initial Reynolds number (figure 2), although there is a slight tendency for the decay rate to decrease with time. Enstrophy decays more rapidly as expected, although the rate is noticeably less than the similarity prediction (dashed line) as previously noted. The similarity transformation (1.1) is also only partially successful in collapsing the energy spectra (figure 3*b*). As later spectra lie to the right in the similarity coordinates, the evolution is slower than predicted at all wavenumbers. Self-similarity on a different timescale does not appear to be out of the question however.

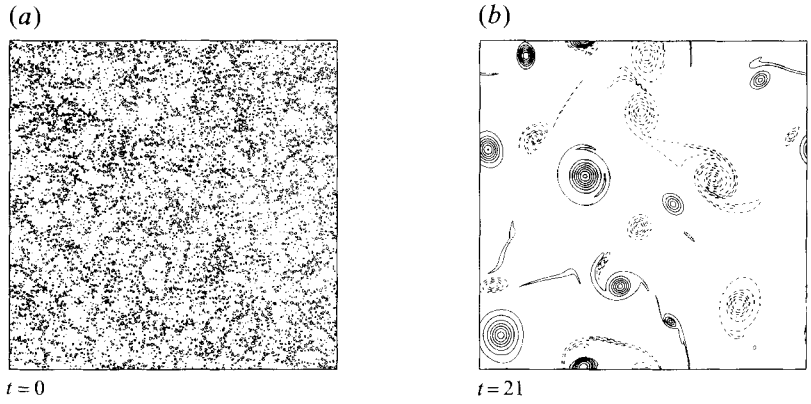


FIGURE 1. (*a*) Initial vorticity. (*b*) Final vorticity.

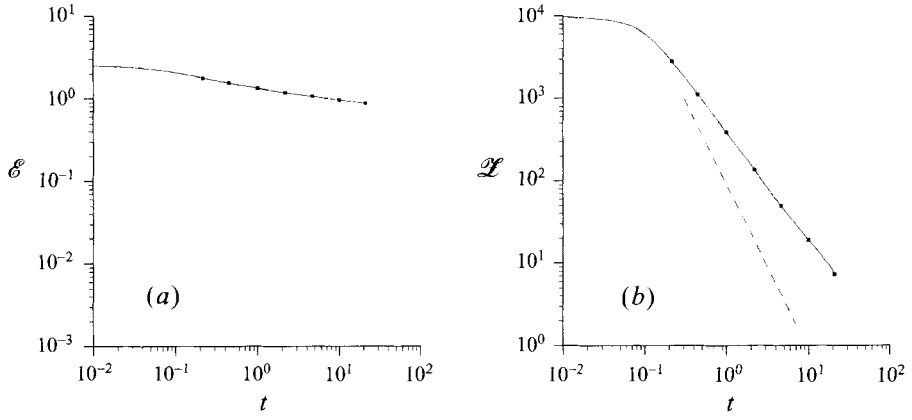


FIGURE 2. (*a*) Energy $\mathscr{E}$ *vs. t.* (*b*) Enstrophy $\mathscr{Z}$ *vs. t.* The dashed line corresponds to the $t^{-2}$ similarity law. The dots indicate the sampling times, $T_i$, listed in table 1.

By contrast, the one-point velocity density, obtained by binning collocation-grid values into 501 intervals, is nearly time invariant as predicted (figure 4*a*). This is particularly true at intermediate times when the integral scale is not too large and the sample density is not too noisy. The density is close to Gaussian and narrows slowly as energy decays. The invariance is also noticeably improved when similarity variables, defined by the instantaneous energy, are used (figure 4*b*).

The one-point vorticity distribution also narrows significantly with time (figure 5*a*), an indication that the Reynolds number of the Navier–Stokes simulation is too low to demonstrate convincingly that the amplitude of the most intense vortices is conserved. The density does appear to be self-similar over a range of vorticity however, beyond which it falls off rapidly (figure 5*b*). Also, the range of the similarity variable $\omega t$, over which self-similarity applies, appears to increase with time (since the extrema decay more slowly than $t^{-1}$). The value of $p_\omega$ also falls off slowly in the self-similar region just above the tails (as seen in log-log coordinates in figure 6*a*), suggesting that the normalized field is becoming increasingly intermittent and non-Gaussian with time.

The hyperviscosity simulation is similar in most respects except that energy is now more nearly conserved whereas enstrophy decays even more slowly, presumably

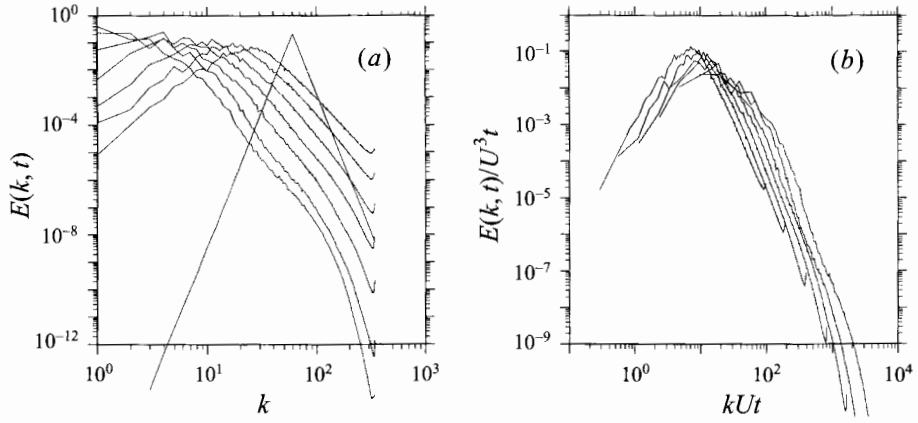


FIGURE 3. (*a*) Energy spectrum for $t = 0$ (triangular curve) and $t = T_i$. Later curves are shifted to the left. (*b*) In terms of similarity variables. Later curves are shifted to the right.

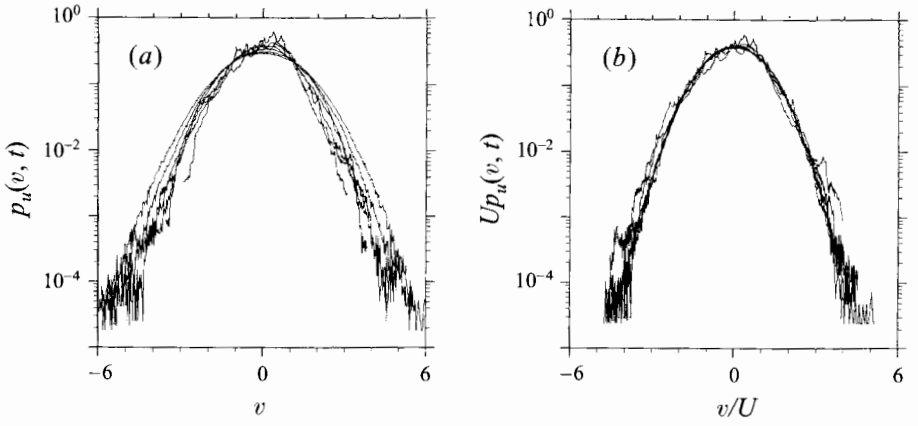


FIGURE 4. (*a*) One-point velocity distribution for $t = T_i$. Later curves are narrower. (*b*) In terms of similarity variables using instanteous energy.

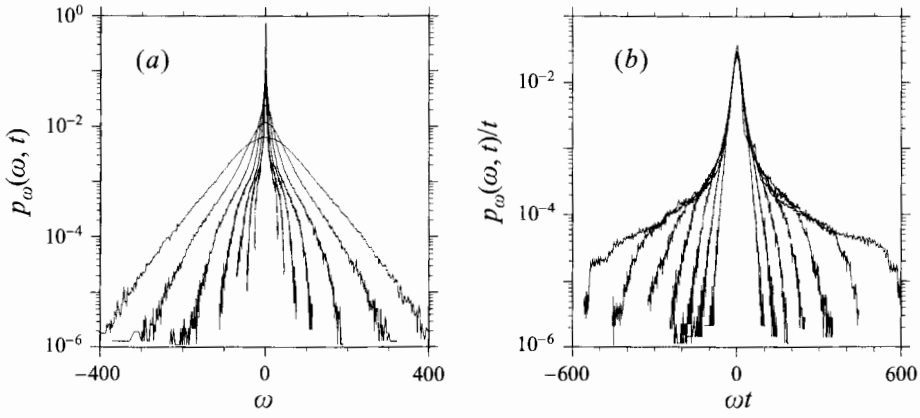


FIGURE 5. (*a*) One-point vorticity density at times $t = T_i$. The density narrows with time. (*b*) In terms of similarity variables. The scaled density broadens with time.

| $T_i$ | $\mathscr{E}$ | $\mathscr{Z}$ | $N_t$ |
|---|---|---|---|
| 0 | 2.55 | 10,000 | 0 |
| 0.22 | 2.52 | 6,874 | 20 |
| 0.47 | 2.49 | 3,631 | 38 |
| 0.99 | 2.47 | 1,696 | 64 |
| 2.15 | 2.46 | 1.001 | 104 |
| 4.61 | 2.45 | 712 | 175 |
| 9.99 | 2.44 | 558 | 309 |

TABLE 2. Hyperviscosity simulation ($\nu_8 = 10^{-39}$).

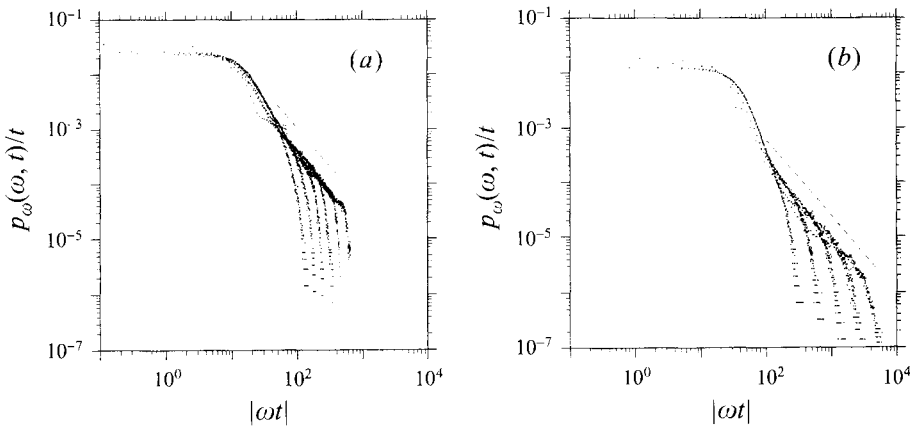


FIGURE 6. One-point vorticity density in log-log coordinates. (*a*) Navier–Stokes. (*b*) Hyperviscosity. The reference lines have slopes of −1.4.

because of the higher effective Reynolds number (table 2). Similarity again fails for both the enstrophy decay rate and the energy spectrum but holds for the velocity density and central portion of the vorticity density. The latter is noisier however (figure 6b). The vorticity density is again found to narrow with time but much more slowly, suggesting that the amplitude of the most intense vortices is more nearly conserved. The dimensionless similarity range increases even more quickly with time so that the normalized field becomes even more intermittent.

There are differences between the two simulations (figure 6): while both vorticity densities appear to exhibit power-law behaviour above the tails with similar slopes, the peak of the hyperviscosity density is about a factor of 2 lower and the power-law range begins at somewhat larger values of $\omega t$. This may be due to the form of the dissipation operator although residual Reynolds number effects cannot be discounted.

Other simulations suggest that the enstrophy decay rate and vorticity moments of the Navier–Stokes simulations depend on the initial conditions and Reynolds number, whereas the velocity density and scaled central core of the vorticity density are relatively insensitive to these factors.

## 3. The vorticity distribution

After an initial transient period $p_\omega$ appears to obey Batchelor scaling for $|\omega| < \omega_m(t)$, while it falls off rapidily in the transient tails. The rapidity of the fall-off in the

tails also appears to increases with time in similarity variables, suggesting that the density can be approximated by the truncated expression

$$p_\omega(\omega,t) \sim \begin{cases} t f(\omega t), & |\omega| < \omega_m \\ 0, & |\omega| > \omega_m, \end{cases} \tag{3.1}$$

which is a special case of the generalized similarity (1.7). The bound $\omega_m$ is evidently a measure of the amplitude of the most intense vortices in the field (possibly excluding rare and inconsequential 'outliers' associated with the transient tails) and so should in some sense be analogous to the McWilliams' (1990) invariant $\zeta_{ext}$, exploited by Carnevale *et al.* (1991). In other words, $\omega_m$ should be invariant for large Reynolds numbers.

Since

$$\langle|\omega|^q\rangle \sim 2t^{-q}\int_0^{\omega_m t} x^q f(x)\,\mathrm{d}x \tag{3.2}$$

and since $\omega_m t$ should increase with time, there are two possibilities: either

(i)

$$I_q(\omega_m t) = \int_0^{\omega_m t} x^q f(x)\,\mathrm{d}x$$

converges for all $q$ as $\omega_m t \to \infty$, in which case the dependence on $\omega_m$ drops out. Batchelor's hypothesis and (1.3) then hold (although this could take some time to develop if $f$ is broad). Otherwise

(ii) $I_q$ diverges for $q > q_c$ as $\omega_m t \to \infty$ (it is emphasized that $p_\omega$ is truncated, not $f$). In this case similarity is recovered when $q < q_c$ and spoiled for $q > q_c$. Given the failure of the enstrophy decay law this is the most likely possibility, at least when $q \geqslant 2$. In fact, since the (scaled) density appears to be hyperbolic (figure 6), i.e.

$$f \sim c/2|x|^{1+q_c}$$

as $|x| \to \infty$, where $c$ and $q_c \doteq 0.4$ are universal, similarity appears to be spoiled for all moments $q > q_c$.

It is, of course, always possible that similarity will be recovered after sufficient time, although no such tendency has ever been observed. In fact, the slopes of the higher-order moments (figure 7*a*) decrease slightly near the end of the Navier–Stokes simulation, suggesting that the departures from similarity are actually increasing (although the domain size could also be a factor).

Since $f$ can be divided into two ranges, $p_\omega$ has three distinct parts: a self-similar central core $|\omega| < x^*/t$, a self-similar intermediate hyperbolic range $x^*/t < |\omega| < \omega_m$ and weak transient tails for $|\omega| > \omega_m$. Here, $x^*$ denotes the beginning of the hyperbolic range of $f(x)$. In the Navier–Stokes simulation we estimate that $x^* = 70 \pm 10$.

## 4. Vorticity moments

### 4.1. *Modified similarity*

If $f$ is hyperbolic, all moments of $f$ of order $q > q_c$ diverge, while the vorticity moments exhibit a phase transition†

$$\langle|\omega|^q\rangle \sim \begin{cases} c_q\, t^{-q}, & -1 < q < q_c \\ c\, \ln(\omega_m t)\, t^{-q_c}, & q = q_c \\ c\,(q-q_c)^{-1}\, \omega_m^{q-q_c}\, t^{-q_c}, & q > q_c, \end{cases} \tag{4.1}$$

† Here the term 'phase' is used in the thermodynamic sense of coexisting phases of a substance.

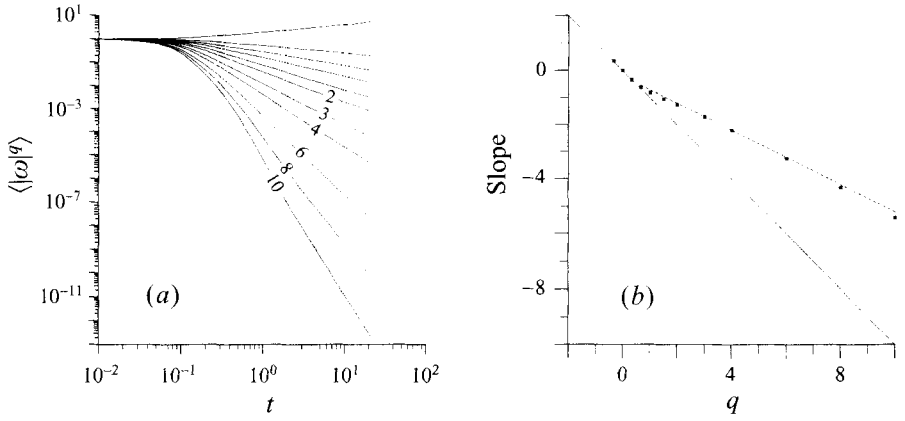


FIGURE 7. (*a*) Vorticity moments *vs.* $t$ for $q = -\frac{1}{3}, \frac{1}{3}, \frac{2}{3}, 1, 1\frac{1}{2}, 2, 3, 4, 6, 8$ and 10, normalized by the value at $t = 10^{-2}$. (*b*) Slopes of (*a*) measured over the range $2.1 \leqslant t \leqslant 21$. The solid line corresponds to similarity while the dashed line is $t^{-a_q}$ with $a_q = 0.2 + 0.5q$.

as $t \to \infty$ between the self-similar 'sea' and the coherent vortices, where $c_q$ represents the (convergent) moments of $f$. Moments of order $q < q_c$ consequently obey Batchelor scaling, while those of order $q > q_c$ are similar in form to (1.5) on setting $q_c = \xi/2$. Equation (4.1) has the advantage that it is dimensionally consistent and the $q$-dependence of the prefactors is explicit for $q \geqslant q_c$. Note that while both expressions (1.5) and (4.1) predict $q$-independent decay rates, they differ in their dependence on the invariant by a factor $\omega_m^{-q_c}$, if $\omega_m$ and $\zeta_{ext}$ are identified (or proportional). It is argued later that this is probably related to the fact that the vortex properties are not narrowly distributed at large times, as assumed in the vortex theory.

Equations (4.1) and (1.5) both predict smaller enstrophy decay rates and hence enhanced energy dissipation, i.e. $t^{-q_c}$ (with $q_c \doteq 0.4$) versus $t^{-2}$, so that the net (i.e. time-integrated) dissipation is unbounded as $t \to \infty$. In other words, even though the Reynolds number of the energy-containing scales increases in time, the energy dissipation ultimately becomes important at large times, presumably driving the system towards a state of rest (unless the Reynolds number is infinite initially).

### 4.2. *Comparison with simulations*

The vorticity moments of the Navier–Stokes simulation scale reasonably well with time as

$$\langle|\omega|^q\rangle \sim t^{-a_q} \tag{4.2}$$

(figure 7*a*), although a close examination indicates some curvature in the higher-order moments. The moments exhibit a clear phase transition at small $q$, where they agree with the Batchelor prediction

$$a_q = q$$

(figure 7*b*, solid line). By contrast, the decay rate of the higher-order moments is linear in $q$, i.e.

$$a_q \doteq 0.2 + 0.5q \tag{4.3}$$

in apparent contradiction with (4.1). This is explained if $\omega_m$ decays due to finite Reynolds number effects. Thus if we follow Weiss & McWilliams (1993) and take

$$\omega_{\mathrm{m}} \sim t^{-\eta}$$

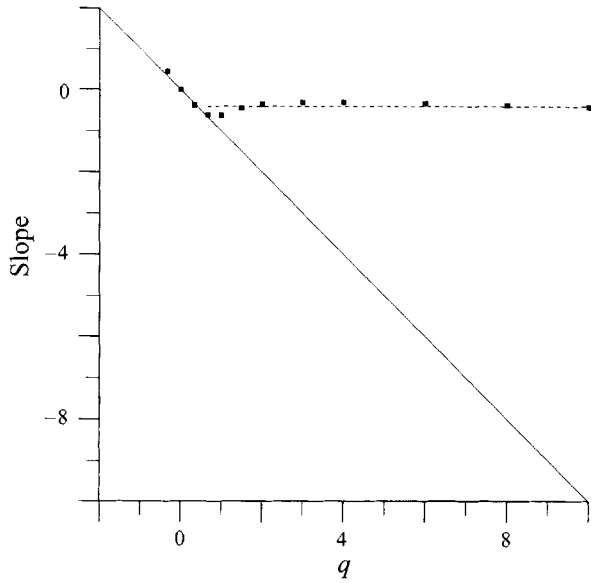


FIGURE 8. Same as figure7(*b*) but for hyperviscosity. The dashed line corresponds to $t^{-0.4}$.

then (4.1) gives (4.2) with

$$a_q = (q - q_c)\eta + q_c,$$

i.e. a power-law decay of $\omega_m$ induces a linear $q$-dependence. Furthermore, (4.3) is recovered on taking $\eta = 0.5$. In other words *both* constants are determined by choosing a *single* parameter (direct support for power-law decay of $\omega_m$ and $\eta = 0.5$ is also given below). Note however that when (1.5) is used in place of (4.1) then

$$a_q = q\eta + \xi/2,$$

which cannot be made to agree with (4.3) for any choice of $\eta$.

The vorticity moments of the hyperviscosity simulation also scale with time but are somewhat noisier. They also exhibit a clear phase transition and Batchelor similarity for $q < q_c$, while

$$a_q \doteq 0.4 \tag{4.4}$$

for the higher-order moments (figure 8), i.e. the exponent is independent of $q$ and equal to $q_c$ as expected when $\omega_m$ is invariant.

We have also attempted to measure $\omega_m$ directly using

$$\Phi \equiv \frac{q - q_c}{q - 1 - q_c} \frac{Z_q}{Z_{q-1}},$$

which according to (4.1) tends to $\omega_m$ for $q > q_c$. $\Phi$ as a function of $q$ at different times for the Navier–Stokes simulation is shown in figure 9(*a*). $\Phi$ decays with time (reflecting the decay of $\omega_m$) and is independent of $q$ only for large $q$ at early times while it is independent of $q$ for all $q$ at large times. This is expected since the moments will converge to (4.1) only when the hyperbolic range is long enough to ensure that the main contribution comes from $\omega \sim \omega_m$. At early times the range is too short so (4.1) holds only for large $q$. At later times the range is long and (4.1) holds for all $q > q_c$.

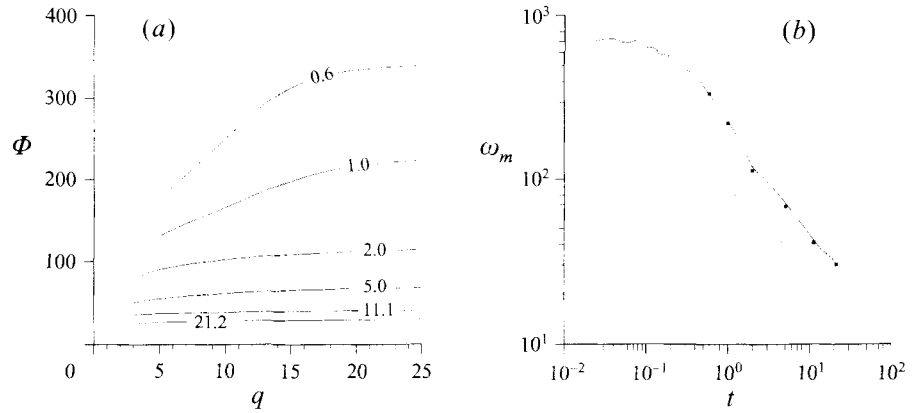


FIGURE 9. (*a*) $\Phi$ *vs.* $q$ at time $t = 0.6, 1, 2, 5, 11.1, 21.2$. $\Phi$ decreases with time. (*b*) $\omega_e = \max(|\omega|)$ (curve) and $\Phi(q = 25, t)$ (dots) *vs.* $t$. The dashed line corresponds to $t^{-0.5}$.

The value of $\omega_m$, estimated from $\Phi(q = 25, t)$ is seen to decay as $t^{-0.5}$ (figure 9*b*), as required in (4.3). Also shown is the extreme value of the vorticity field $\omega_e = \max(|\omega|)$. The fact that $\omega_e$ is only slightly larger than $\omega_m$ is a little worrying given that the sample moments are expected to be reliable estimates of ensemble averages only when they are not dominated by a few extrema. Note also that $\omega_e$ does not decay monotonically early on in the Navier–Stokes simulation as it should, indicating that the dissipation range is under-resolved initially (figure 3). The long-time evolution is thought to be accurate however, as energy begins to cascade upscale. A similar procedure applied to the hyperviscosity simulation is found to be consistent with conservation of $\omega_m$.

### 4.3. *Energy spectrum*

As already noted, figure 3(*b*) suggests that the energy spectrum may be self-similar on a different timescale. If we suppose that $E(k, t)$ depends on $t$ only in the combination $t\, g(\omega_m t)$, i.e. if (1.6) can be written

$$E = U^3 t\, g(\omega_m t)\, F\big(kUtg(\omega_m t)\big),$$

then the only form that is consistent with (4.1) at $q = 2$ is

$$E(k, t) = \frac{U^3 t}{(\omega_m t)^\alpha}\, F\left(\frac{kUt}{(\omega_m t)^\alpha}\right), \tag{4.5}$$

where $\alpha = 1 - q_c/2$. While this expression is not as well-founded as those for the vorticity density and moments, it turns out to be quite effective in collapsing the spectra of the Navier–Stokes simulation (figure 10*a*). It is less succesful for the hyperviscosity simulation however, particularly at low wavenumbers (later curves lie to the left).

## 5. The vortices and the sea

It is tempting to associate the hyperbolic range of the vorticity density with the spectrum of vortex amplitudes or equivalently

$$\omega_s = x^*/t$$

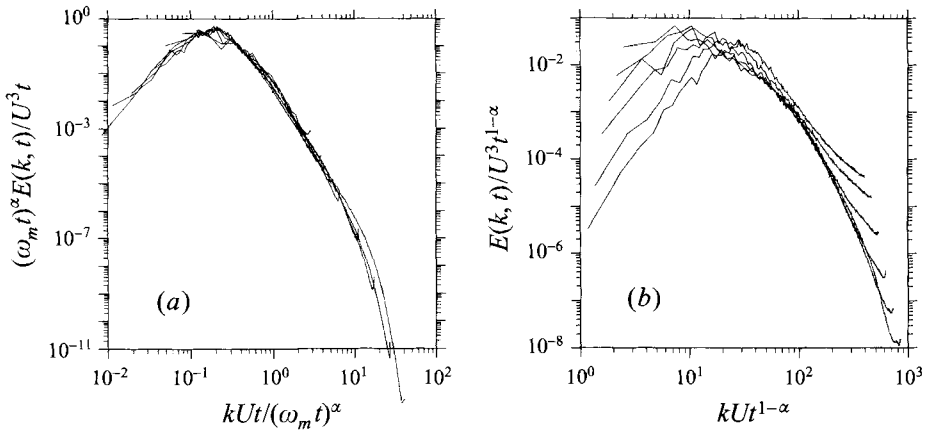


FIGURE 10. Energy spectra at times $T_i$ in terms of modified similarity variables. (*a*) Navier–Stokes. (*b*) Hyperviscosity.

with 'mean sea-level' which separates the vortices from the filamented background. If this is the case, then the vorticity density cannot be explained by a narrowly distributed collection of vortices with top-hat or Gaussian profiles, since the vorticity in the hyperbolic range is too plentiful.† The conjecture is confirmed to some extent by the fact that the universal contours $100/t$ and $10/t$, straddling sea-level ($\doteq 70/t$) lead to a reasonable separation between vortices and filaments throughout the evolution (figure 11). Note that each panel consists of only *two* contours of $\omega$. Since there are residual filaments in panels (*a*) and (*c*) and a few vortices in (*b*) and (*d*), the separation holds only in some average sense.

According to this interpretation there is a spectrum of vortices with amplitudes in the range

$$\omega_s < |\omega| < \omega_m,$$

which increases with time due to the continual production of ever weaker vortices that are either left behind as the sea decays away, or are residuals of interactions between stronger vortices. Vortex production in the sea is expected if the flow is self-similar. In any case, the spectrum of vortex amplitudes appears to broaden with time, possibly explaining the discrepancies between (4.1) and the narrow-band prediction (1.5).

Also since

$$A(\omega_1) = \text{Prob}(|\omega| > \omega_1)$$

represents the fractional area occupied by fluid with vorticity greater than $\omega_1$, the area occupied by vortices with amplitudes greater than a *fixed* threshold

$$A(\omega_1) = c/q_c(\omega_1 t)^{q_c}$$

decays with time as observed in the vortex census of McWilliams (1990). On the other hand, the total area occupied by all vortices

$$A(x^*/t) = c/q_c x^{*q_c}$$

is constant in time. Apparently, losses incurred during the mergers of larger vortices are compensated by the continual production of ever smaller vortices of order $x^*/t$.

† As noted by a reviewer, a field of Gaussian vortices with a single size and amplitude gives $p_\omega \sim \omega^{-1}$ which is too shallow to explain the observed density.

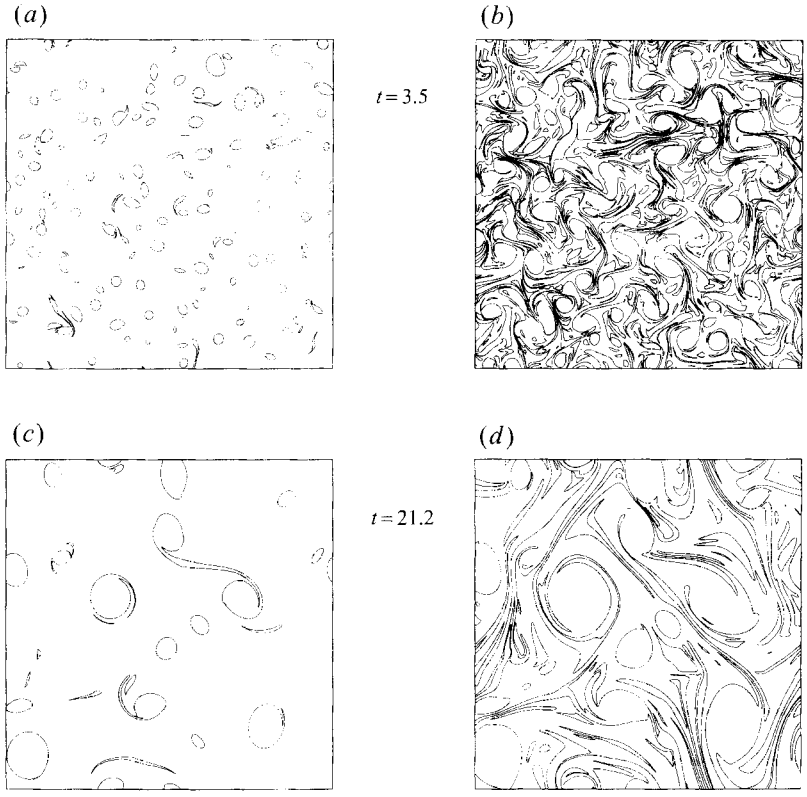


FIGURE 11. Universal vorticity contours: (*a*) $|\omega| = 100/t$, $t = 3.5$; (*b*) $|\omega| = 10/t$, $t = 3.5$; (*c*) $|\omega| = 100/t$, $t = 21.2$; (*d*) $|\omega| = 10/t$, $t = 21.2$.

Like the Batchelor prediction for the vorticity density, the 'sea-level' is 'super universal' in the sense that it is totally independent of the properties of the flow.

## 6. Final remarks

Our results suggest that while Batchelor's similarity hypothesis fails to describe some aspects of decaying two-dimensional turbulence, it succeeds for others. In particular, it holds for the one-point velocity distribution, the central portion of the one-point vorticity density, and low-order vorticity moments. It fails for higher-order moments, essentially because the underlying universal density is hyperbolic and, in a sense, describes an infinite enstrophy flow. Equivalently, the failure can be attributed to the existence of a second rugged invariant, which can either be associated with the support of the vorticity density or the amplitude of the strongest vortices. All vorticity moments continue to scale with time but exhibit a phase transition. The higher-order moments depend on the second invariant and are similar in form to those predicted by the vortex model of Carnevale *et al.* (1991) in that the decay rates are independent of the order. There are differences however, particularly with regard to the dependence on the invariant, presumably because the vortex properties do not remain narrowly distributed as $t \to \infty$ for flows on unbounded domains. In particular, it is found that there is an expanding spectrum of vortices with amplitudes in the

range $\omega_s \leqslant |\omega| \leqslant \omega_m$, where the lower bound $\omega_s \doteq 70/t$ defines 'mean sea level', the threshold separating the vortices from the background sea.

Our description as well as that of Carnevale *et al.* (1991) is based on the existence of a second rugged invariant, $\omega_m$, in the high-Reynolds-number limit, which to date has only been observed in hyperviscosity simulations. Given its potential significance, additional theoretical and numerical confirmation of the invariant should be a priority. The extent to which two- and higher-point statistics can be explained also remains an open question.

We appreciate helpful comments expressed by D. Straub and the anonymous reviewers. The second author would also like to acknowledge support from the Natural Sciences & Engineering Research Council of Canada.

## REFERENCES

BASDEVANT, C., LEGRAS, B., SADOURNY, R. & BÉLAND, M. 1981 A study of barotropic model flows: intermittency, waves and predictability. *J. Atmos. Sci.* **38**, 2305–2326.

BATCHELOR, G. K. 1969 Computation of the energy spectrum in two-dimensional turbulence. *Phys. Fluids Suppl. II.* **12**, 233–239.

BENZI, R., COLLETA, M., BRISCOLINI, M. & SANTANGELO, P. 1992 A simple point vortex model of two-dimensional decaying turbulence. *Phys. Fluids* A **4**, 1036–1039.

BENZI, R., PALADIN, G., PATARNELLO S., SANTANGELO, P. & VULPIANI, A. 1986 Intermittency and coherent structures in two-dimensional turbulence. *J. Phys.* A: *Math. Gen.* **19**, 3771–3784.

BENZI, R., PATARNELLO, S. & SANTANGELO, P. 1987 On the statistical properties of two-dimensional decaying turbulence. *Europhys. Lett.* **3**, 811–818.

BENZI, R., PATARNELLO, S. & SANTANGELO, P. 1988 Self-similar coherent structures in two-dimensional decaying turbulence. *J. Phys.* A: *Math. Gen.* **21**, 1221–1237.

CARNEVALE, G. F., MCWILLIAMS, J. C., POMEAU, Y., WEISS, J. B. & YOUNG, W. R. 1991 Evolution of vortex statistics in two-dimensional turbulence. *Phys. Rev. Lett.* **66**, 2735–2737.

CARNEVALE, G. F., POMEAU, Y. & YOUNG, W. R. 1990 Scaling theory for ballistic merger problems. *Phys. Rev. Lett.* **64**, 2913.

FORNBERG, B. 1977 A numerical study of two-dimensional turbulence. *J. Comput. Phys.* **25**, 1–31.

HUBER, G. & ALSTRØM, P. 1993 Universal decay of vortex density in two dimensions. *Physica* A **195**, 448–456.

LILLY, D. K. 1969 Numerical simulation of two-dimensional turbulence. *Phys. Fluids Suppl. II* 240–249.

MARIOTTI, A., LEGRAS, B. & DRITSCHEL, D. 1994 Vortex stripping and the erosion of coherent structures in two-dimensional flows. *Phys. Fluids* **6**, 3954–3962.

MCWILLIAMS, J. C. 1984 The emergence of isolated coherent vortices in turbulent flow. *J. Fluid Mech.* **146**, 21–43.

MCWILLIAMS, J. C. 1990 The vortices of two-dimensional turbulence. *J. Fluid Mech.* **219**, 361–385.

SANTANGELO, P., BENZI, R. & LEGRAS, B. 1989 The generation of vortices in high resolution, two-dimensional decaying turbulence and the influence of initial conditions on the breaking of self-similarity. *Phys. Fluids* A **1**, 1027–1034.

WEISS, J. B. & MCWILLIAMS, J. C. 1993 Temporal scaling behaviour of decaying two-dimensional turbulence. *Phys. Fluids* A **5**, 608–621.